Adsorption of Organosulfur Species at Aqueous Surfaces: Molecular Bonding and Orientation

Teresa L. Tarbuck and Geraldine L. Richmond*

Materials Science Institute and Department of Chemistry, University of Oregon, Eugene, Oregon 97403

Received: April 13, 2005; In Final Form: August 25, 2005

Four sulfur-containing compounds important to tropospheric chemistry have been examined at the vapor/H_2O and vapor/D_2O interfaces. These adsorbates, DMS, DMSO, $DMSO_2$, and $DMSO_3$, were studied by surface tension and vibrational sum-frequency spectroscopy (VSFS). Each adsorbate is surface active and each orients with the hydrophobic methyl groups pointed out of the plane of the interface. Their influence on the interfacial water structure is adsorbate dependent. Strong and weak interactions with surface water are observed as well as reorientation of subsurface water molecules, resulting in an increase in interfacial thickness.

Introduction

Sulfur-containing aerosol particles play an important role in global climate through their interaction with solar and terrestrial radiation. Some prevent energy from reaching the Earth's surface (the white house effect) and some trap heat radiating from the Earth indirectly by acting as cloud condensation nuclei. The size and composition of these particles influence the formation of clouds and affect the rates of chemical reactions in the atmosphere.

Of the wide range of organic constituents in aerosol particles, the sources, sinks, and photochemistry of compounds in the sulfur cycle are the least understood.[1] Anthropogenic and nonanthropogenic contributions are of similar orders of magnitude, with much of the nonanthropogenic sulfur contribution arising from the decay of organic matter and from sea spray. Dimethyl sulfide (DMS) produced by metabolic processes in certain algae is the largest natural source of sulfur in the troposphere.[2] Some of its oxidation products found in the atmosphere are dimethyl sulfoxide (DMSO), dimethyl sulfone ($DMSO_2$), methane sulfonic acid (MSA), carbonyl sulfide (COS), and sulfur dioxide (SO_2). Generally, sulfur compounds influence climate by acting as cloud condensation nuclei, by scattering radiation, and/or by modifying cloud properties. For example, DMSO strongly scatters light in the troposphere, whereas long-lived COS can be transported to the stratosphere and, through oxidation, affect the concentration of ozone.

Sulfur-containing aerosols in the troposphere are mainly comprised of water, dissolved salts, and other adsorbed organic compounds. Their structure resembles that of a reverse micelle.[3] Organic, hydrophobic molecules are more concentrated at the surface, and the interior is primarily composed of water and dissolved salts. These aerosols provide a medium in which compounds can react both at the surface and in the interior.

As models for the surface of sulfur-containing aerosol particles, DMS, DMSO, $DMSO_2$, and $DMSO_3$ were examined at the vapor/water interface. The orientations of these adsorbates and their effects on water structure were examined to gain better insight into their influence on the chemical and physical properties of aerosol particles in the nonanthropogenic tropospheric sulfur cycle. These compounds are small organic molecules with hydrophobic methyl groups and hydrophilic sulfur and oxygen atoms. The number of oxygen atoms in the molecule affects the geometry (see Figure 1) and electron distribution in these compounds, resulting in very different physical properties. For example, DMS is less dense than water and evaporates quickly from the water surface, while DMSO is hygroscopic and completely miscible in water. Although these adsorbates are different physically, they are all surface active at the vapor/water interface. Studies of the acidity trend of these compounds have shown that the addition of oxygen increases destabilization by withdrawing charge and thereby increasing acidity.[4] Aside from their atmospheric effects, each compound is important in other areas of chemistry. For example, $DMSO_2$ is used as a solvent in chemical reactions. DMSO has a number of medical uses and is the most commonly studied molecule in this series, with several recent molecular dynamics (MD) simulations providing structural, thermodynamic, and dynamic insight into the properties of the vapor/DMSO/water interface.[5,6]

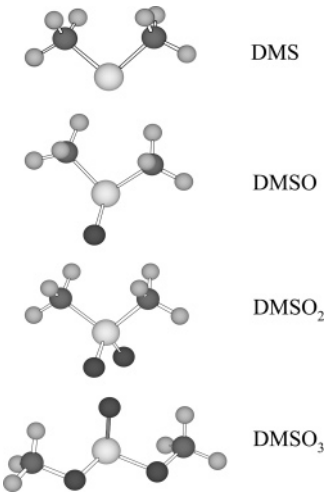

Figure 1. Ball and stick models for each of the compounds (DMS, DMSO, $DMSO_2$, and $DMSO_3$) studied. Black = oxygen, dark gray = carbon, medium gray = hydrogen, light gray = sulfur.

In these studies, surface concentrations, adsorbate−adsorbate interactions, and the influence of adsorbates on the water structure is presented. The water structure at the vapor/water interface is seen to change in various ways that accommodate each of the four adsorbates with similarities between DMS and $DMSO_3$ and between DMSO and $DMSO_2$. This study builds

10.1021/jp058123z CCC: $30.25
Published on Web 10/15/2005

on and clarifies previous work in this laboratory with respect to DMSO.[7,8]

Background. Vibrational sum-frequency spectroscopy (VSFS) is an ideal technique for studying liquid interfaces because it is a surface-specific (bulk contributions are forbidden based on symmetry) vibrational technique that gives insights into bonding strengths, orientation, and coordination of interfacial molecules. There is currently significant literature available on the technique.[9−17]

The sum-frequency intensity is the square of the second-order susceptibility, $\chi^{(2)}$, which is a sum of all resonant modes and a nonresonant mode. Sum-frequency spectra are fit to deconvolve the resonant modes. To take into account the inhomogeneous broadening and the homogeneous line widths of the vibrational transitions, a fitting routine first proposed by Bain[18] is employed:

$$\chi^{(2)} = \chi_{\mathrm{NR}}^{(2)} e^{i\varphi} + \sum_{\nu} \int_{-\infty}^{+\infty} \frac{A_\nu e^{i\phi_\nu}\, e^{-[\omega_{\mathrm{L}} - \omega_\nu/\Gamma_\nu]^2}}{\omega_{\mathrm{IR}} - \omega_{\mathrm{L}} + i\Gamma_{\mathrm{L}}} \mathrm{d}\omega_{\mathrm{L}} \qquad (1)$$

The first term is the nonresonant second-order susceptibility, χ_{NR}. The second term sums all resonant modes. It includes the convolution of the homogeneous line width of the transition (HWHM, Γ_{L}) with inhomogeneous broadening (fwhm, $\sqrt{2\ln 2}\Gamma_\nu$) and a transition strength, A_ν, which is proportional to the product of the number of molecules and their orientationally averaged IR and Raman transition probabilities. The frequency of the IR, the Lorentzian, and the resonant mode are ω_{IR},ω_{L},and ω_ν, respectively.

Intensity changes in the sum-frequency spectrum as a function of concentration can be attributed to a change in the number of interfacial molecules, a change in molecular orientation, and/or a change in bond strength. For sum-frequency intensity dependence on concentration, the number of molecules at the surface at each concentration can be compared to the second-order resonant susceptibility. Equation 2 shows this relationship:

$$\chi_{\mathrm{R}}{}^{(2)}(\nu) = \frac{N}{\epsilon_0}\langle\beta_\nu\rangle \qquad (2)$$

The resonant susceptibility is proportional to N, the number of molecules contributing to the sum-frequency response, and $\langle\beta_\nu\rangle$, the orientationally averaged molecular susceptibility. If the relationship between the susceptibility and the number density at the interface is linear, the molecules are not reorienting.

In these experiments, three polarization combinations are utilized: *ssp*, *sps*, and *ppp*. These polarization schemes denote the sum-frequency, visible, and infrared polarizations, respectively, which represent polarizations in the plane of incidence (*p*) and normal to the plane of incidence (s). Transition dipoles that have a component perpendicular to the plane of the interface are probed in *ssp*. Likewise, transition dipoles that have a component parallel to the plane of the interface are probed in *sps*. For liquid systems that are isotropic in the plane (and when the laser beams are far from electronic resonances), the Raman tensor is symmetric; therefore, *sps* and *pss* are the same after correction for the Fresnel coefficients. The *ppp*-polarization scheme is a combination of four $\chi^{(2)}$ elements: $\chi_{XXZ}^{(2)}$, $\chi_{XZX}^{(2)}$, $\chi_{ZXX}^{(2)}$, and $\chi_{ZZZ}^{(2)}$. One way to get at $\chi_{ZZZ}^{(2)}$, the out-of-plane Raman and IR responses, is subtracting $\chi_{XXZ}^{(2)}$, $\chi_{XZX}^{(2)}$, and $\chi_{ZXX}^{(2)}$, from the *ppp*-polarized spectrum. This is difficult in practice unless the Fresnel coefficients are accurate for all wavelengths. The *ppp*-polarization scheme is useful in that it can serve as a check of the *ssp*- and *sps*-polarization features.

Surface Tension. Surface tension measurements are a useful tool for acquiring the number density of adsorbates at an interface. When coupled with sum-frequency spectroscopy, one can determine whether the molecules are reorienting with increasing surface density from a plot of the square root of the SF intensity versus the number density at the interface. Intensity changes that vary linearly with the number density would be indicative of a lack of reorientation.

Surface pressure isotherms are fitted to the Gibb's equation:[19]

$$\Gamma_i = \frac{1}{nRT}\left(\frac{\partial\pi}{\partial \ln(a_i)}\right)_T \qquad (3)$$

to obtain the maximum surface excess. Γ_i is the surface excess concentration at maximum surface coverage, π is the surface pressure, n is the number of species in excess, and a_i is the activity. For low concentrations, the activity can be replaced with the bulk concentration. With the maximum surface excess (Γ_i) and the Frumkin equation:[19]

$$\pi_2 = -RT\Gamma_i \ln\left[1 - \frac{\Gamma_2}{\Gamma_i}\right] \qquad (4)$$

the surface excess for each bulk concentration can be determined. π_2 is the surface pressure for each bulk concentration, and Γ_2 is the surface excess for each surface pressure. For each solution, the contribution from the bulk concentration and the surface excess are summed to give the total surface concentration.

Experimental Section

Laser System. The laser system has been described extensively in previous publications.[20,21] Therefore, only a brief overview is given here. The sum-frequency light is generated by overlapping 800 nm (2 ps, 1 kHz repetition rate) and tunable (2700−4000 cm^{-1}) infrared light in a copropagating geometry. Intensities are ∼100 μJ of 800 nm light and 4−10 μJ of IR at 56° and 67° from the surface normal, respectively. After filtering reflected 800 nm light, sum-frequency light is collected every 0.0025 μm over the tunable range with a thermoelectrically cooled CCD camera (Princeton Instruments). The samples implied are poured or injected via gastight syringes into glass dishes that are enclosed in a Telfon cell fitted with CaF_2 windows.

Sample Preparation and Analysis. The sulfur compounds, DMS (99+%), DMSO (99.9%, HPLC grade), $DMSO_2$ (98%, lot analysis 99.8%), and $DMSO_3$ (99%) were purchased from Aldrich and used as received. D_2O (d99.9%) was purchased from Cambridge Isotopes. High-purity H_2O was obtained from a Millipore Nanopure system (17.6 MΩ cm). Because of the volatility and solubility of DMS and $DMSO_3$, these solutions were injected into 8.25 mL of water via a gastight syringe. DMSO and $DMSO_2$ samples were prepared by weight in advance. The bulk water is ∼8 mm thick, isolating the effects of the glass/water interface from the vapor/water interface.

All spectra are divided by the nonresonant response from an unprotected gold surface over the same frequency range. The normalization eliminates variations in the SF intensity due to spatial variation between the visible and IR beams when scanning the IR frequencies, the temporal lengthening of the pulses by water vapor, and the optics used for filtering the sum-frequency. Because of the volatility of DMS, large adsorbances of IR energy in the CH stretching region are present. The DMS

spectra are divided by a nonresonant gold spectrum taken in the sample cell containing water and DMS.

As discussed earlier, the interference between overlapping vibrational modes and between the nonresonant intensity and the vibrational modes lead to a more complex analysis strategy relative to linear surface spectroscopies. The parameters used to fit the neat vapor/water interface in *ssp*-polarization are taken from previous isotopic dilution studies.[22−24] These studies iteratively fit spectra of pure H_2O, various concentrations of D_2O in H_2O (HOD), and pure D_2O. This allowed all the spectra to be fit with the same peak positions, Lorentzian widths, phases, and similar Gaussian widths. Lorentzian widths were fixed at 2, 5, and 12 cm^{-1} for the CH, OH, and free OH modes, respectively. The phase relationships are consistent with those seen in molecular dynamics simulations of the neat interface.[22,25] At the neat water interface, the free OH and high-frequency stretching modes (>3600 cm^{-1}) are out of phase with the lower frequency (<3500 cm^{-1}) modes. Except for the free OH, the Gaussian widths are broad, 100−135 cm^{-1}. The parameters used to fit the neat vapor/water interface in *sps*-polarization are similar to the parameters used for the *ssp*-polarization spectrum with the exception of an additional resonance at $\sim$3580 cm^{-1}.

Concentrations and concentration ranges of the adsorbates employed in this study provided spectra of high reproducibility. For DMS, high bulk concentrations ($\sim 3 \times 10^{-3}$ bulk mole fraction) were required to maintain a constant surface concentration during spectral acquisition. DMSO is completely miscible in water and was studied over the entire concentration range. $DMSO_2$ is less soluble and was also studied over its entire concentration range (to $\sim$0.04 *X*). $DMSO_3$ is less volatile than DMS, and its effect on the water structure is more pronounced, therefore, spectra at lower concentrations ($0.6-3.0 \times 10^{-4}$ *X*) were acquired.

Surface Tension. Surface tension measurements were performed using the Wilhelmy plate method.[26−28] Surface coverages were determined using activities for DMSO[29,30] and mole fractions for $DMSO_2$ and $DMSO_3$. The volatility of DMS prevented reproducible determination of quantitative surface concentrations. The surface tension of DMSO has been previously recorded in this laboratory[7] over all mole fractions of DMSO in water, and the present results are comparable.

Results and Discussion

The results of surface tension measurements, including surface concentrations and the limiting area per molecule for certain bulk adsorbate concentrations of DMSO, $DMSO_2$, and $DMSO_3$, are presented first. The presentation and discussion of VSF spectra of DMS, DMSO, $DMSO_2$, and $DMSO_3$ at the vapor/D_2O and the vapor/H_2O interface in *ssp*- and *sps*-polarizations follows. The adsorbates are discussed in pairs based on spectral similarities. DMS and $DMSO_3$ are presented together, as are DMSO and $DMSO_2$. The discussion includes: spectral assignments for the adsorbates, determination of adsorbate orientation and adsorbate−adsorbate interactions from the vapor/adsorbate/D_2O spectra, spectral assignments for neat water, and finally, an analysis of the effect of each adsorbate on interfacial water structure.

Surface Tension. Surface tension measurements were conducted for three of the four surface active species, DMSO, $DMSO_2$, and $DMSO_3$, to acquire surface concentrations for use in the spectral analysis. Although consistent surface tension measurements could not be acquired for DMS because of its volatility, DMS is assumed to be surface active due to the hydrophobic methyl groups and a dipole moment that does not increase with solvation. The number of molecules at the surface, as a function of the bulk mole fraction for concentrations below 0.3 bulk mole fraction of DMSO, $DMSO_2$, and $DMSO_3$, are presented in Figure 2. The data show that the molecules partition to the surface, with $DMSO_3$ having the greatest surface activity. The inset in Figure 2 expands the surface concentration data of $DMSO_3$ bulk concentrations and shows that the surface concentration for $DMSO_3$ starts to plateau at $\sim 3 \times 10^{14}$ molecules/cm^2 (or $\sim 3 \times 10^{-4}$ bulk mole fraction). At 3×10^{-4} bulk *X*, 97% of the total surface concentration is due to the surface excess. DMSO and $DMSO_2$ are less surface active. For $DMSO_2$, the surface concentration does not plateau and its low solubility (to $\sim$0.04 bulk mole fraction) limits the number of data points taken. Similarly, DMSO surface concentrations do not plateau. This adsorbate is the least surface active with surface concentrations around 3×10^{14} molecules/cm^2 at much higher bulk concentration ($\sim$0.2 bulk mole fraction) than $DMSO_3$. Table 1 shows the limiting areas per molecule, $\sim 21 \pm 5$, 50 ± 5, and 31 ± 15 $Å^2$/molecule for DMSO, $DMSO_2$, and $DMSO_3$, respectively. For DMSO, this is consistent with previous surface tension[7] and molecular volume analysis[31] results of $\sim$19 and 24 $Å^2$/molecule, respectively. The area per molecule for $DMSO_3$ is the most difficult to determine because the surface tension changes dramatically over a comparatively small concentration range ($0.6-3.0 \times 10^{-4}$ bulk *X*). For DMSO, $DMSO_2$, and $DMSO_3$, the limiting area per molecule is reached at approximately 1.0, 0.04, and 0.0004 *X*, respectively. Also shown in Table 1 is the surface concentration for these molecules at a bulk concentration that is representative of the spectra shown below.

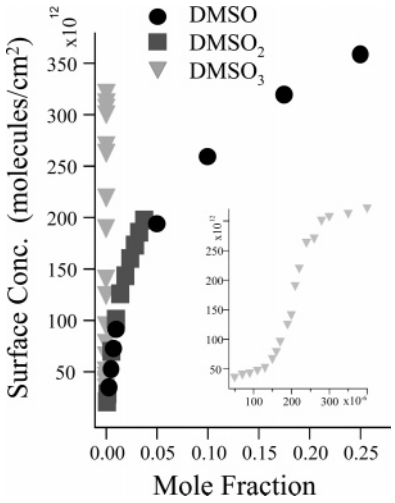

Figure 2. The surface concentrations at the interface for bulk mole fractions of DMSO (●), $DMSO_2$ (■), and $DMSO_3$ (▲). The inset expands the bulk mole fractions for $DMSO_3$ (▲).

TABLE 1: Surface Tension Results for the Adsorbates Including the Surface Coverage for the Representative Spectra and the Maximum Surface Coverage

adsorbate	bulk conc (mf)	surface conc (molecules/cm^2)	max number density ($Å^2$/molecule)
DMS	0.003	[a]	[a]
DMSO	0.01	9.1×10^{13}	21 ± 5
$DMSO_2$	0.02	1.5×10^{14}	50 ± 5
$DMSO_3$	0.0002	1.4×10^{14}	31 ± 15

[a] The volatility of DMS prevented reproducible determination of surface concentrations.

Adsorbate Spectral Assignments. Figure 3a and b show representative VSF spectra of DMS and $DMSO_3$ (Figure 3a) and DMSO and $DMSO_2$ (Figure 3b) at the vapor/D_2O interface.

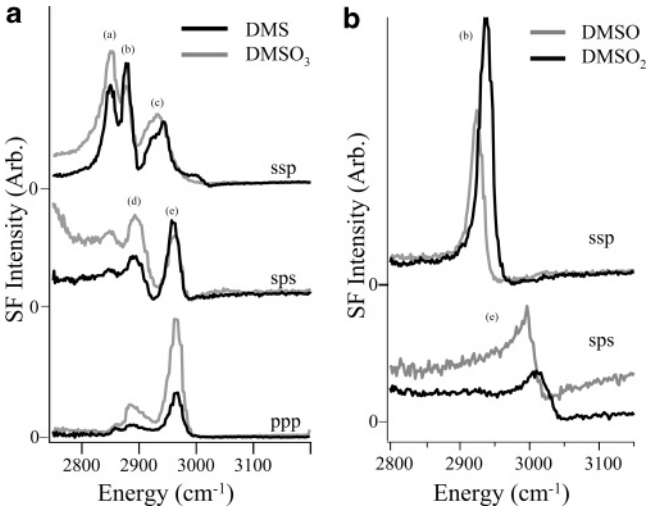

Figure 3. (a) DMS and $DMSO_3$ (4×10^{-3} and 2×10^{-4} bulk *X*, respectively) in the C−H stretching region at the vapor/D_2O interface acquired under *ssp*-, *sps*-, and *ppp*-polarizations. (a, b, c, d, e) Methyl overtone deformation, a methyl symmetric stretch, a methyl Fermi resonance, a methyl overtone deformation, and a methyl antisymmetric stretch, respectively. Uncertainties in the sum-frequency modes are ±5 wavenumbers. (b) Sum-frequency spectra of DMSO and $DMSO_2$ (both concentrations are 0.02 bulk *X*) at the vapor/D_2O interface acquired under *ssp*-polarization (top) and *sps*-polarization (bottom), where concentrations of DMSO are 0.20 bulk *X* and $DMSO_2$ 0.03 bulk *X*. Uncertainties in the sum-frequency modes are ±5 wavenumbers.

TABLE 2: Vibrational Assignments for VSFS Peaks in the C−H Stretching Region from Spectral Fits to *ssp* and *sps* Data at the Vapor/D_2O Interface (Energies Are in cm^{-1})

adsorbate	CH_3def	CH_3SS	CH_3FR	CH_3def	CH_3AS
DMS[a]	2858	2882	2935	2903	2966, 3000
DMSO		2917−2927			2995−3007
$DMSO_2$		2942			3020
$DMSO_3$	2858	2882	2935	2910	2966
labels	(a)	(b)	(c)	(d)	(e)

[a] DMS has two antisymmetric stretches at 2966 and 3000 cm^{-1} of A_1 and B_2 symmetry, respectively. Energies are obtained from spectral fits to the data in Figure 3a and b. DMSO frequencies blue-shift with increasing water concentration.

The active sum-frequency modes (methyl overtones, symmetric stretches, and Fermi resonances) in the CH stretch region are presented in Table 2. The sum-frequency spectra of DMS and $DMSO_3$ are more complicated and have more features than DMSO and $DMSO_2$ because they exhibit a number of deformation overtones with the same symmetries and similar frequencies as a number of methyl stretches in the spectral region displayed.

DMS and $DMSO_3$ have common spectral features in *ssp*- and *sps*-polarizations: a CH_3 overtone of a deformation mode (2858 cm^{-1}), a methyl symmetric stretch (2882 cm^{-1}), another overtone deformation (∼2903 and 2910 cm^{-1}, respectively), a Fermi resonance (2935 cm^{-1}), and a methyl antisymmetric stretch (2966 cm^{-1}). Following previous work, the Fermi resonance pairs that appear at 2882 and 2935 cm^{-1} are assigned as a symmetric stretch and a Fermi resonance.[32−35] DMS also has an additional methyl antisymmetric stretch (3000 cm^{-1}) present in *ssp*-polarization. These modes are assigned based on a collection of IR and Raman mode assignments for vapor,[36−38] polycrystalline,[39] and liquid[37,40,41] samples. The sum-frequency modes are similar in wavelength to bulk liquid IR and Raman frequencies.

Sum-frequency spectral assignments for DMSO and $DMSO_2$ are also presented in Table 2. The methyl symmetric stretch (CH_3−SS) and the methyl antisymmetric stretch (CH_3−AS) for DMSO are at 2917 and 2995 cm^{-1}, respectively. DMSO is completely miscible in water, and the center frequency of the methyl symmetric and methyl antisymmetric stretch blue-shift with increasing water concentration. Previous work from this laboratory[7] suggested that the symmetric stretch for pure DMSO was at 2903 cm^{-1}. Improved normalization techniques and fitting procedures that include a nonresonant feature now indicate that the symmetric stretch of the CH_3 group is at ∼2917 cm^{-1} for the surface of pure DMSO, consistent with IR (2917 cm^{-1}) and Raman (2913 cm^{-1}) bulk frequencies.[42]

$DMSO_2$ is soluble over a small concentration range (to ∼0.04 *X*), and the frequency of the CH_3−symmetric stretch (2942 cm^{-1}) does not change significantly over this range. This frequency agrees with the Raman frequency (2944 cm^{-1}) for various concentrations in distilled water.[43] The methyl antisymmetric stretch occurs at 3023 cm^{-1} for $DMSO_2$ and is similar to IR and Raman frequencies of the pure molten sample, 3022 and 3018 cm^{-1}, respectively.[44]

Adsorbate Orientation. Adsorbate orientations are deduced from the SF spectra of the vapor/adsorbate/D_2O interface for DMS, DMSO, $DMSO_2$, and $DMSO_3$ in the CH stretching region. Because the IR transition moments for the methyl symmetric and antisymmetric stretches are perpendicular to each other, a qualitative comparison of the total intensity of these modes (in any polarization scheme) gives information about the orientation of the adsorbate. Spectral similarities, molecular orientation, and adsorbate−adsorbate interactions of DMS and $DMSO_3$ are discussed first, followed by DMSO and $DMSO_2$. Finally, comparisons of all four adsorbates are made.

VSF spectra of DMS and $DMSO_3$ at the vapor/D_2O interface were acquired in *ssp*-and *sps*-polarization as shown in Figure 3a. Vibrational modes with transition moments perpendicular to the plane of the interface are probed in *ssp*-polarization. IR transition moments parallel to the interface are probed in *sps*-polarization. The presence of a strong methyl symmetric stretch and Fermi resonance and the absence of a strong methyl antisymmetric stretch in *ssp*-polarization for DMS and $DMSO_3$ indicate that the hydrophobic methyl moieties have an average orientation with a significant component perpendicular to the surface plane. The *sps*-polarization data show no symmetric stretch intensity, and the methyl antisymmetric stretch at ∼2966 cm^{-1} dominates the spectrum providing additional support for this conclusion. However, there is a small contribution from both the methyl deformation overtone (at 2903 cm^{-1} for DMS and 2910 cm^{-1} for $DMSO_3$) and the methyl antisymmetric stretch (2966 cm^{-1}) in *ssp*-polarization. The large tail of the CH_3 deformation overtone (2858 cm^{-1}) in Figure 3 is an interference between the deformation overtone and the tails of the free OD and other OD vibrations centered at ∼2740 and 2550 cm^{-1}, respectively. These OD vibrations interfere with the CH stretching vibrations because the adsorption of these molecules at the vapor/D_2O interface enhances the OD stretching intensities.

Spectra of DMS and $DMSO_3$ are also shown in *ppp*-polarization. The sum-frequency intensity in *ppp*-polarization is a sum of four $\chi^{(2)}$ elements and their respective Fresnel coefficients, squared: $I_{ppp} \propto |f\chi^{(2)}_{XXZ} + f\chi^{(2)}_{XZX} + f\chi^{(2)}_{ZXX} + f\chi^{(2)}_{ZZZ}|^2$. Spectra in this polarization scheme contain all the SF resonant modes and, therefore, are used to confirm the mode position and assignments presented in Table 2. Because there are several CH modes, fitting the same modes in several polarization schemes minimizes the uncertainty in the relative phases of the modes and in the peak positions. The strongest features are the

methyl symmetric and methyl antisymmetric stretches for both compounds, and this polarization scheme reveals the similarities between these two interfaces.

In contrast, the interfaces of *neat* DMS and $DMSO_3$ have very different SF spectra. For neat DMS in *ssp*-polarization (not shown), the SF spectral features are weak, but they resemble bulk IR and Raman spectra (both symmetric and antisymmetric stretching are present). The strongest feature in the neat $DMSO_3$ *ssp*-polarization sum-frequency spectrum is a strong CH_3-AS at $\sim$2957 cm^{-1}, similar to bulk IR and Raman spectra for neat $DMSO_3$. This is in contrast to the strong CH_3-SS in *ssp*-polarization for both DMS and $DMSO_3$ at the vapor/water interface. Clearly, the addition of water greatly changes the orientation of both compounds at the surface. This suggests that water induces orientation of the adsorbates due to the hydrophobic methyl groups.

DMSO and $DMSO_2$ at the vapor/D_2O interface in *ssp*-polarization are shown in Figure 3b. These spectra at 0.02 *X* show one strong vibrational resonance, the methyl symmetric stretch. The strong methyl symmetric stretch (and lack of antisymmetric stretch) for both compounds indicates that the hydrophobic methyl groups are oriented out of the plane of the interface. The *sps*-polarization spectra of DMSO and $DMSO_2$ at the vapor/D_2O interface have one dominant feature, the methyl antisymmetric stretch. The appearance of the antisymmetric stretch (and lack of the symmetric stretch) complements the *ssp*-polarization data showing that, on average, the CH_3 moiety is oriented out of the plane of the interface.

Changes in orientation with increasing bulk concentration were investigated for the adsorbates, but could not be determined quantitatively for DMS. Qualitatively, the resonant modes in the DMS spectra (not shown) change proportionally with increasing concentration, and a strong methyl symmetric stretch is observed throughout the concentration series. This suggests that there is minimal change in orientation with concentration for DMS. $DMSO_3$ displays the longest surface equilibration time, allowing the adsorption and reorientation of $DMSO_3$ to be monitored spectroscopically in time. For example, the CH_3 deformation overtone is the strongest feature when $DMSO_3$ is spread onto the surface, but it decreases with time, while the methyl symmetric and Fermi resonance grow in intensity and eventually dominate the methyl deformation overtone. $DMSO_3$ is the only adsorbate that shows a significant change in orientation with concentration. Figure 4a shows a concentration series with the spectral fits for $DMSO_3$ in *ssp*-polarization. This concentration series ranges from 0.6 to 3.0×10^{-4} bulk *X* and surface concentrations extend from $\sim 3.5 \times 10^{13}-3.4 \times 10^{14}$ molecules/cm^2 (or $\sim$290$-$31 $Å^2$/molecule). The fitted sum-frequency peak areas are compared with the surface tension results. Figure 5 shows the square roots of the SF intensities for each concentration against the corresponding surface concentrations. Referring back to eq 2, a linear relation exists between the second-order susceptibility and the surface concentration if the orientationally averaged molecular susceptibility does not change. The deviation of the $DMSO_3$ data from linearity is attributed to changes in orientation associated with crowding due to the increasing $DMSO_3$ concentration.

For DMSO, the data and spectral fits for the concentration series from 0.005 to 1.0 bulk *X* (surface concentrations from $5 \times 10^{13}-4.9 \times 10^{14}$ molecules/cm^2 corresponding to 190$-$21 $Å^2$/molecule) are shown in Figure 4b. The frequency for the symmetric stretch in *ssp*-polarization ranges from 2927 cm^{-1} for 0.005 *X* to 2917 cm^{-1} for pure DMSO, a 10 cm^{-1} blue-shift with increasing water concentration. Similarly, the anti-

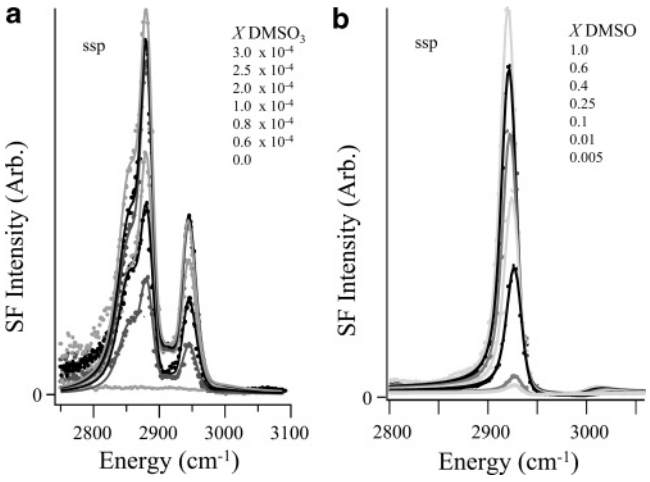

Figure 4. (a) Sum-frequency spectra with spectra fits of $DMSO_3$ in the C$-$H stretch region at the vapor/D_2O interface acquired under *ssp*-polarization from bottom to top: neat D_2O, 0.6×10^{-4} *X*, 0.8×10^{-4} *X*, 1.0×10^{-4} *X*, 2.0×10^{-4} *X*, 2.5×10^{-4} *X*, 3.0×10^{-4} *X*. (b) Sum-frequency spectra with spectral fits of DMSO in the C$-$H stretch region at the vapor/D_2O interface acquired under *ssp*-polarization from bottom to top: 0.005 *X*, 0.01 *X*, 0.1 *X*, 0.25 *X*, 0.4 *X*, 0.6 *X*, 1.0 *X*.

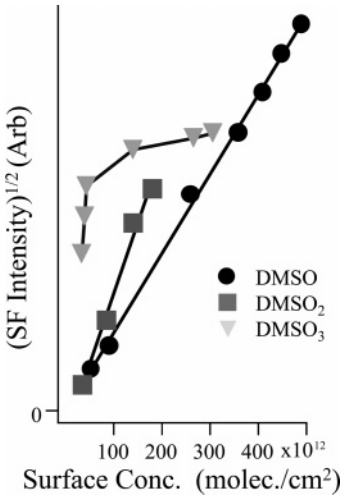

Figure 5. Square root of the sum-frequency intensity versus the surface concentration for DMSO (●), $DMSO_2$ (■), and $DMSO_3$ (▲) for the same bulk concentrations shown in Figure 4a and b.

symmetric stretch in *sps*-polarization ranges from 3007 to 2995 cm^{-1}, a 12 cm^{-1} blue-shift. This blue-shift with increasing water concentration has been observed previously in this laboratory[7] and investigated recently by several groups[45−47] in experiments and MD simulations of bulk solutions and DMSO/water clusters. In this SF study, the spectra show the methyl CH bond strength increasing throughout the range of DMSO concentrations examined. We attribute this to a change in CH bond strength due to DMSO$-H_2O$ interactions. The CH bonds would contract due to the change in electron distribution when water molecules bind to the oxygen of DMSO and when water molecules solvate DMSO. The role of the electrostatic field of hydrating water molecules and the role of the electron density rearrangement that lead to observed spectral blue-shifts are discussed in several simulation studies.[47−53] Sum-frequency intensities as a function of surface concentration (Figure 5) show a linear relationship for DMSO and indicate that reorientation does not occur. Although self-association of DMSO and crowding effects are possible at higher bulk concentrations,[7,29] the surface methyl groups do not show signs of reorientation in the present study. These results for DMSO are in agreement with recent resonance

TABLE 3: Summary of Results and Conclusions

adsorbate	bulk conc *X*	surface conc molecules/cm^2	surface excess divided by total surface conc	avg methyl orientation	prominent effect of the adsorbate−water interaction
DMS[a]	0.003	*a*	*a*	into the vapor	cooperative H_2O-H_2O vibrations are enhanced
DMSO	0.1	2.6×10^{14}	15%	into the vapor	strong bonding between DMSO−H_2O
$DMSO_2$	0.03	1.8×10^{14}	56%	into the vapor	H_2O orientation becomes random
$DMSO_3$	0.0003	3.1×10^{14}	97%	into the vapor	interfacial depth increases

[a] The volatility of DMS prevented reproducible determination of surface concentrations.

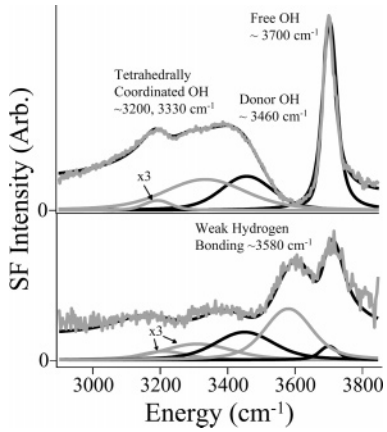

Figure 6. Sum-frequency spectra of the vapor/water interface acquired under *ssp*- and *sps*-polarizations. Fitted peaks are shown below the spectra.

enhanced surface second harmonic studies for mole fractions below 0.1.[54] In the case of $DMSO_2$, the CH_3 symmetric stretch does not change frequency with increasing concentration. $DMSO_2$ also shows a linear relationship in Figure 5. $DMSO_2$ is soluble over a small concentration range (to ~0.04 *X*). Surface concentrations are below $\sim 2 \times 10^{14}$ molecules/cm^2 or greater than ~50 Å^2/molecule. At these concentrations, crowding effects between $DMSO_2$ molecules are not expected and reorientation does not occur.

For all four adsorbates present, the orientations of the molecules are such that the methyl groups are, on average, out of the plane of the interface. At low surface concentrations, the adsorbates are widely spaced and adsorbate−absorbate interaction is minimal. With increasing surface concentration, DMSO and $DMSO_2$ do not reorient; however, $DMSO_3$ does reorient with increasing surface coverage. As the area per molecule is reduced, the $DMSO_3$ molecules reorder due to crowding and interactions with other $DMSO_3$ molecules. The major results and conclusions in this section are collected in Table 3. Table 3 also previews results and conclusions for the following sections.

Water Assignments. A spectrum of the neat vapor/water interface in *ssp*-polarization is shown in Figure 6 (top). The fitted resonant modes of the spectrum are shown. As mentioned earlier, the parameters used to fit the neat vapor/water interface in *ssp*-polarization were obtained from isotopic dilution studies.[22,24] The nonresonant component (not shown) has been taken into account in the analysis. OH stretching modes are assigned based on the degree of hydrogen bonding and the surrounding environment.[22,55,56] As the amount of cooperative OH stretching between adjacent water molecules increases, the vibrational frequency decreases. From right to left, the first spectral feature is at ~3700 cm^{-1} and is attributed to the unbound OH (free OH) stretch of a water molecule straddling the interface. Its vibrational motion is uncoupled from the other OH vibration (donor OH) in the molecule. This donor OH can hydrogen-bond to other water molecules and appears at lower frequency (~3460 cm^{-1}).[24] Intensity from the symmetric OH stretching of water in an asymmetric hydrogen-bonding environment also appears in this region. Last, OH stretching of tetrahedrally coordinated water molecules occurs at ~3330 and 3200 cm^{-1}. These assignments are supported by IR and Raman data from bulk water that assign the strong intensity in the 3200−3450 cm^{-1} range to stretching of tetrahedrally coordinated water molecules in various hydrogen-bonding environments.[57−60]

An *sps*-polarization spectrum of the neat vapor/water interface is shown in Figure 6 (bottom). The neat vapor/water interface in *sps*-polarization is consistent with that published by Wei and Shen[61] and shows much lower SF intensity over the entire OH stretching region. The intensities of the two spectra are not directly comparable, but the lower signal-to-noise for the *sps*-polarization spectrum is evident. The features present in the *sps*-polarization spectra are the same as those seen in the *ssp*-polarization spectra, with an additional resonance at ~3580 ± 50 cm^{-1}. The phase of this peak has not been determined experimentally; therefore, the uncertainty in the frequency is large. Bonded species are assumed to have a component directed toward the bulk, and MD simulations[25] show the phase changing in this 3600 cm^{-1} region. Given the high frequency of the mode, we do not expect it to be from highly coordinated OH species, but rather from species with few hydrogen bonds. We assign this peak to symmetric OH stretching of weakly hydrogen-bonded water molecules. This frequency range (3520−3650 cm^{-1}) includes OH stretching in an asymmetric environment,[57] antisymmetric OH stretching, and water molecules with fewer hydrogen bonds (double donors), which give prominent OH stretches in cluster studies.[62−64]

Water Structure. A basic understanding of the neat vapor/water interface has been established by recent sum-frequency studies in combination with X-ray adsorption spectroscopy, neutron diffraction, and molecular dynamics simulations. Free OH oscillators are estimated to comprise approximately 20% of the interface,[56] with each free OH contributing one donor OH. The remainder of the interface is comprised of species with 2−4 hydrogen bonds, including donor and acceptor water molecules[65] and various tetrahedrally coordinated OH oscillators. The orientations of the free OH oscillators are out of the plane of the interface, and molecular dynamics simulations[23,25,66] have shown that the orientation of the dipole at the interface is close to the interfacial plane and slightly inward toward the bulk. X-ray absorption spectroscopy indicates that the intermolecular oxygen−oxygen distance undergoes an expansion as one moves from the bulk to the surface.[67] Results from molecular dynamics[23,68] indicate that the interfacial depth is small, ~6−9 Å, and the average coordination of water molecules decreases from ~3.6 bonds per molecule in the bulk to ~2 bonds per molecule near the interface.[68]

Effect of Adsorbates on Water Structure. The effects of DMS (3×10^{-3} *X*) and $DMSO_3$ (0.6×10^{-4} *X*) on the vapor/H_2O interface in *ssp*-polarization are shown in Figure 7a. There are several changes that occur with the addition of each adsorbate, most noticeably the loss of the sharp free OH and

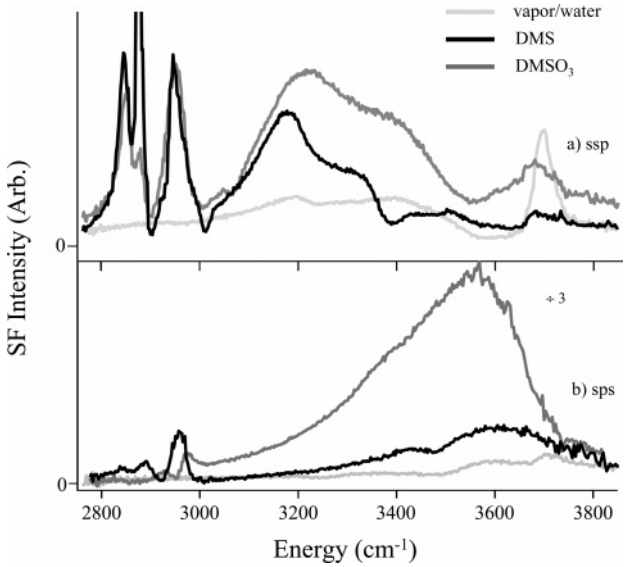

Figure 7. Sum-frequency spectra of DMS and $DMSO_3$ at the vapor/water interface in the C−H and O−H stretching regions. (a) *ssp*-polarization spectra of the neat vapor/water interface, 4×10^{-3} bulk *X* DMS, and 0.8×10^{-4} bulk *X* $DMSO_3$. (b) *sps*-polarization spectra of the vapor/water interface with 4×10^{-3} bulk *X* DMS and 2×10^{-4} bulk *X* $DMSO_3$. The spectrum of the vapor/$DMSO_3$/water interface is scaled by 1/3.

an increase in intensity around 3200 cm^{-1} in the symmetric tetrahedrally hydrogen-bonded OH stretching region. This increase in intensity in the 3200 cm^{-1} region results in significant interference between the OH and CH stretching regions, which can be unraveled by spectral fitting. The only way to preserve the frequencies of the adsorbate's CH peaks from the D_2O interface at the H_2O interface is to shift the phase in the coordinated OH stretching region by 180°. This 180° phase change indicates that coordinated water molecules at this adsorbate/water interface are reorienting from a dipole orientation that is slightly toward the bulk to an orientation that is toward the gas phase. Interestingly, upon solvation, the dipole moments of DMS and $DMSO_3$ are very different in strength ~1.7 and 4 D, respectively; and yet, both of these adsorbates strongly orient water, demonstrating that the dipole moment of the adsorbate is not the sole predictor of the ability to orient surface water molecules.

In the *sps*-polarization spectra of adsorbed DMS and $DMSO_3$ (Figure 7b), the high-frequency features (the donor and weak hydrogen bonding at 3460 and 3580 cm^{-1}, respectively) are the most prominent OH stretching features. The enhancement in the high-frequency OH modes has been observed in other *sps*-polarization spectra of oriented organic adsorbates at the air/water interface.[32] Additionally, the weakly bonded OH resonance at ~3590 cm^{-1} for the DMS/water interface is blue-shifted compared to the neat vapor/water interface (~3580 cm^{-1}). This feature is red-shifted to ~3550 cm^{-1} for the $DMSO_3$/water interface, which suggests the $DMSO_3$−water interaction is stronger than the DMS−water interaction. The greater strength of hydrogen bonding between $DMSO_3$ and water is not surprising because $DMSO_3$ is large, polarizable, and has more hydrogen-bonding sites.

Although DMS and $DMSO_3$ both change the orientation and enhance the coordinated OH stretching at the interface, $DMSO_3$ significantly increases the depth of the interface. There are several spectral features supporting this interpretation. Both *ssp*- and *sps*-polarization spectra show increases in OH stretching intensity throughout the spectrum even at low bulk concentrations (0.6×10^{-4} *X*). SF spectra at higher bulk concentrations show even more enhancement across the OH stretching region. For example, the *sps*-polarization spectrum of $DMSO_3$ in Figure 7b is scaled (divided by 3) because of the large increase in intensity over most of the OH stretching region. In this spectrum, the OH stretching modes clearly interfere with the methyl antisymmetric stretch, showing that the amplitudes of the OH stretches, even in *sps*-polarization where the signals are generally weak, extend well into the CH stretch region. Similar broad enhancements have been seen in several other studies where an increase in interfacial potential was present.[32,69] Also, as the surface concentrations of $DMSO_3$ increase, a corresponding decrease in the OH oscillators at the interface might be expected as they are crowded and replaced. Instead, the OH stretching modes are enhanced.

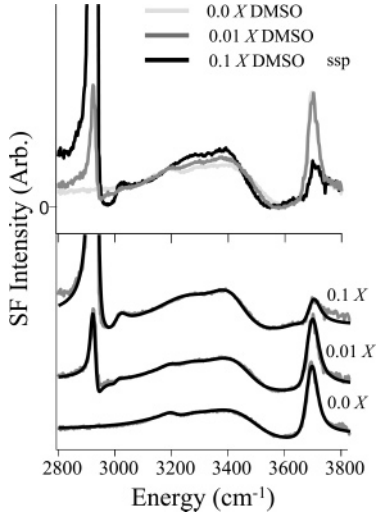

Figure 8. Sum-frequency spectra of DMSO at the vapor/water interface in the C−H and O−H stretching regions in *ssp*-polarization for pure water, 0.01 *X*, 0.10 *X*, and 1.0 *X* DMSO. The top shows the relative spectral intensities and the bottom shows the fits to each spectrum, which have been offset for clarity.

In summary, the presence of DMS and $DMSO_3$ result in an increase in the amplitude and phase change in the symmetric stretch modes of coordinated water molecules (3200, 3330 cm^{-1}), clearly indicating that water molecules are being oriented. $DMSO_3$ significantly broadens the interfacial region, resulting in large increases in these intensities, and the data suggest that the interaction between $DMSO_3$ and water is much stronger than the DMS and water interaction.

The effects of DMSO and $DMSO_2$ on the neat vapor/water interface in *ssp*-polarization are shown in Figures 8 and 9, respectively. Each figure is divided between overlaid spectra at various concentrations (top) and the fits to the spectra (bottom), which are offset. At concentrations below 0.002 *X*, the effect of each adsorbate in the OH stretching region is not detectable. Surface tension measurements at these low concentrations show the molecules partitioning to the surface (the surface concentration is greater than the 2D bulk density),[7,31] even though the water structure as seen in the OH stretching region remains the same. This is very different from DMS and $DMSO_3$, where the reorientation of water molecules and OH coordinated stretching are prevalent at low bulk concentrations.

With increasing bulk concentration, DMSO and $DMSO_2$ have slightly, but measurably, different effects on the water structure. Because the changes from the neat vapor/water interface are small in comparison to the two other adsorbates, the fits are shown and described in more detail. For 0.01 and 0.1 *X* DMSO (Figure 8), the area per molecule is ~110 and 39 $Å^2$,

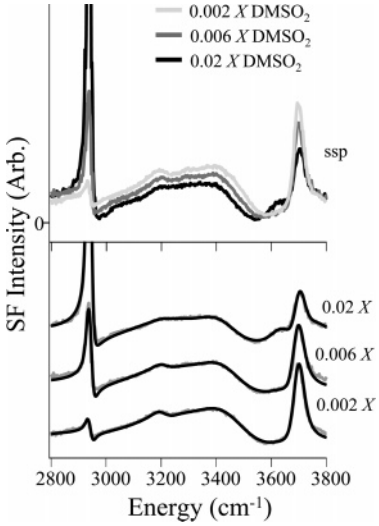

Figure 9. Sum-frequency spectra of $DMSO_2$ at the vapor/water interface in the C−H and O−H stretching regions in *ssp*-polarization for 0.002 *X*, 0.006 *X*, and 0.02 *X* $DMSO_2$. The top shows the relative spectral intensities and the bottom shows the fits to each spectrum, which have been offset for clarity.

respectively. From the fits to the data, the resonant mode at 3200 cm^{-1} does not change, suggesting minimal change in interfacial depth or in symmetric hydrogen-bonding environments of water. The amplitude in the OH stretching region at ∼3330 cm^{-1} increases for DMSO. We attribute this increase to a strong DMSO−water interaction that slightly strengthens the tetrahedral order. The donor OH can either be fit with a red-shift ∼15 and 35 wavenumbers, respectively, to 3445 and 3425 cm^{-1}, compared to the neat water spectrum (3460 cm^{-1}) or a small phase change from π rad to 4 rad (or 180−229°). This indicates small changes in the surface water structure due to either or both water reorienting and hydrogen bond strengthening. There is also a decrease in the free OH mode as DMSO molecules displace surface water molecules. We conclude that DMSO incorporates very well into the water network, causing minimal disruption, consistent with the miscible nature of DMSO and water. Neutron diffraction and MD experiments of bulk DMSO−water mixtures support this interpretation and indicate that water hydrogen-bound to the oxygen in DMSO forms a stronger hydrogen bond than with the oxygen in H_2O.[70−72] The hydrogen-bonding environment was found to be similar to the neat water hydrogen-bonding environment as the local tetrahedral order is preserved.[70,73] At 0.1 *X* and higher, small contributions from an additional OH mode are found from the SF spectral fits at ∼3635 cm^{-1}. This spectral feature is attributed to oriented water-solvating DMSO molecules. Similar solvation features in SF spectra have been reported.[24,74] Recall that effects of water solvation on the CH modes of DMSO were found for this concentration series.

Spectra of $DMSO_2$ at the vapor/water interface in *ssp*-polarization are shown in Figure 9. From the resonant mode analysis, the intensities of the free OH (3700 cm^{-1}), donor OH (3460 cm^{-1}), and coordinated OH stretching (3330 cm^{-1}) all decrease with increasing concentration of $DMSO_2$. This decrease in intensity is attributed to a randomization of water molecules in the interfacial region in the presence of $DMSO_2$. $DMSO_2$ causes a red-shift in the donor OH to ∼3430 cm^{-1} or a small phase change from π rad to 4 rad (or 180−229°) at 0.02 bulk mole fraction. These changes indicate a perturbation of the surface water region without any significant increase in the hydrogen-bonding interactions. The only increase in intensity

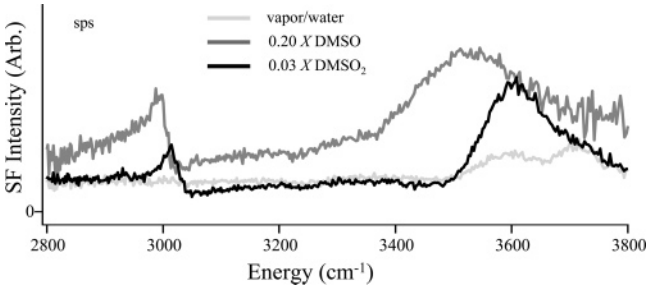

Figure 10. Sum-frequency spectra of DMSO (0.20 *X*) and $DMSO_2$ (0.03 *X*) at the vapor/water interface in the C−H and O−H stretching regions in *sps*-polarization.

with increasing $DMSO_2$ concentration is the OH resonance at ∼3635 cm^{-1}. As in the case of DMSO, this is attributed to interactions typical of oriented water molecules solvating $DMSO_2$.

Figure 10 shows spectra of the neat vapor/water interface, 0.2 *X* DMSO, and 0.03 *X* $DMSO_2$ in the *sps*-polarization scheme. Most of the SF intensity is from the weakly hydrogen-bonded OH resonances that occur at ∼3580, 3550, and 3590 cm^{-1}, for neat H_2O, DMSO, and $DMSO_2$, respectively. A similar weakly bonded feature was reported in Raman studies of bulk DMSO−water mixtures by Scherer et al.[75] Low concentrations (0.05 *X*) of H_2O in DMSO at 80 °C showed a band at 3580 cm^{-1} and the absence of a sharp band near 3682 cm^{-1} (free OH). Scherer et al. proposed that all hydrogen atoms are bonded to some extent (absence of free OH), and this new feature (3580 cm^{-1}) was tentatively assigned to weakly hydrogen-bonded OH stretching vibrations, where both hydrogen atoms of the water molecule are weakly bonded. (Only a small fraction of bulk water appeared to exist in this form at 23 °C.) These high-frequency modes increase with increasing concentration and red- (blue-) shift for DMSO ($DMSO_2$). These data are consistent with the *ssp*-polarization data because DMSO has a stronger hydrogen-bonding interaction with water than $DMSO_2$.

In summary, the presence of DMSO or $DMSO_2$ changes the orientation and/or the strength of hydrogen-bonding interactions with water molecules. Unlike DMSO, which shows tetrahedral coordination similar to neat water and increases in hydrogen-bonding strength, the combination of *ssp*-and *sps*-polarization data for $DMSO_2$ at the vapor/water interface show that the $DMSO_2$−water interaction is comparatively weak.

Conclusions

The surface properties of four tropospheric sulfur compounds, DMS, DMSO, $DMSO_2$, and $DMSO_3$, were examined at the vapor/H_2O interface by sum-frequency spectroscopy and surface tension measurements. The surface concentrations and activities of these compounds, their orientation, and their effects on the structure of water at the vapor/H_2O interface were analyzed.

Each of the four compounds display surface activity. $DMSO_3$ has the greatest surface activity, followed by $DMSO_2$ and DMSO, as measured by surface pressure isotherms. The limiting areas per molecule are 31, 50, and 21 $Å^2$/molecule, respectively, showing that, although DMSO is the least surface active, it forms more tightly packed monolayers than $DMSO_2$.

The orientation of the hydrophobic methyl groups is, on average, out of the plane of the interface for each compound studied, on the basis of *ssp*- and *sps*-polarization data of these compounds at the vapor/D_2O interface. For DMS, DMSO, and $DMSO_3$, small contributions from the methyl antisymmetric stretch are present in *ssp*-polarized spectra, showing that the orientation of the methyl groups, while out of the plane of the

interface, are not aligned along the surface normal. $DMSO_3$ reorients with increasing surface concentration. DMSO and $DMSO_2$ show little or no sign of orientation change with increasing surface concentration. The anomalous blue-shift in frequency of the methyl symmetric stretch of DMSO is attributed to the shortening of the C−H bond due to strong hydrogen bonding with the oxygen of DMSO and to weaker bonding interactions between the methyl hydrogen and water.

All four adsorbates alter the interfacial water structure. Both DMS and $DMSO_3$ reorient water molecules and enhance the hydrogen-bonding interactions between water molecules in the interfacial region. Water−adsorbate interaction for both compounds is also present, with $DMSO_3$ showing a stronger interaction. The increased SF signal observed from water in the presence of $DMSO_3$ is attributed to an expanded interfacial region being probed because of increased surface potential upon adsorption. In comparison, DMSO and $DMSO_2$ orient fewer water molecules even though they have a significant dipole moment. These results indicate that additional factors beyond the molecular dipole contribute to surface water orientation. These include water−solute bonding interactions and the surface orientation of the solute. The interactions between DMSO and water maintain the strength and tetrahedral order in the interfacial region found at the neat vapor/water interface. $DMSO_2$ randomizes water molecules and shows weaker $DMSO_2$−water interactions. DMSO causes a red-shift (and $DMSO_2$ a blue-shift) from the neat vapor/water interface in the high-frequency modes associated with weak hydrogen bonding and double donor modes based on *sps*-polarization data. At higher concentrations of DMSO and $DMSO_2$, features indicative of solvating water molecules (3635 cm^{-1}) are observed.

Extrapolating these results to aerosol particles, our results suggest that these sulfur compounds could be a significant factor in the surface behavior of aqueous aerosols. They clearly partition from the bulk to the surface of aqueous solutions. This enhanced adsorption also alters the bonding behavior of water to different degrees at the surface.

Acknowledgment. We thank the National Science Foundation (CHE 0243856) for supporting this research and the Office of Naval Research for Instrumentation.

References and Notes

(1) Wayne, R. P. *Chemistry of Atmospheres*, 3rd ed.; Oxford University Press: Oxford, 2000.
(2) Bates, T. S.; Lamb, B. K.; Guenther, A.; Dignon, J.; Stoiber, R. E. *J. Atmos. Chem.* **1992**, *14*, 315.
(3) Ellison, B. G.; Tuck, A. F.; Vaida, V. *J. Geophys. Res.* **1999**, *104*, 11633.
(4) Speers, P.; Laidig, K. E.; Streitwieser, A. *J. Am. Chem. Soc.* **1994**, *116*, 9257.
(5) Benjamin, I. *J. Chem. Phys.* **1999**, *110*, 8070.
(6) Senapati, S. *J. Chem. Phys.* **2002**, *117*, 1812.
(7) Allen, H. C.; Gragson, D. E.; Richmond, G. L. *J. Phys. Chem.* **1999**, *103*, 660.
(8) Allen, H. C.; Raymond, E. A.; Richmond, G. L. *Curr. Opin. Colloid Interface Sci.* **2000**, *5*, 74.
(9) Richmond, G. L. *Anal. Chem.* **1997**, *69*, 536A.
(10) Richmond, G. L. *Chem. Rev.* **2002**, *102*, 2693.
(11) Zhu, X. D.; Suhr, H.; Shen, Y. R. *Phys. Rev. B* **1987**, *35*, 3047.
(12) Bloembergen, N.; Pershan, P. S. *Phys. Rev.* **1962**, *128*, 606.
(13) Guyot-Sionnest, P.; Hunt, J. H.; Shen, Y. R. *Phys. Rev. Lett.* **1987**, *59*, 1597.
(14) Shen, Y. R. *The Principles of Nonlinear Optics*; Wiley: New York, 1984.
(15) Shen, Y. R. *Mater. Res. Soc. Symp. Proc.* **1986**.
(16) Bain, C. D. *J. Chem. Soc., Faraday Trans.* **1995**, *91*, 1281.
(17) Eisenthal, K. B. *Chem. Rev.* **1996**, *96*, 1343.
(18) Bain, C. D.; Davies, P. B.; Ong, T. H.; Ward, R. N.; Brown, M. A. *Langmuir* **1991**, *7*, 1563.
(19) Chattoraj, D. K.; Birdi, K. S. *Adsorption and the Gibbs Surface Excess*; Plenum Press: New York, 1984.
(20) Gragson, D. E.; McCarty, B. M.; Richmond, G. L.; Alavi, D. S. *J. Opt. Soc. Am. B* **1996**, *13*, 2075.
(21) Allen, H. C.; Raymond, E. A.; Richmond, G. L. *J. Phys. Chem.* **2001**, *105*, 1649.
(22) Raymond, E. A.; Tarbuck, T. L.; Richmond, G. L. *J. Phys. Chem. B* **2002**, *106*, 2817.
(23) Raymond, E. A.; Tarbuck, T. L.; Brown, M. G.; Richmond, G. L. *J. Phys. Chem. B* **2003**, *107*, 546.
(24) Raymond, E. A.; Richmond, G. L. *J. Phys. Chem. B* **2004**, *108*, 5051.
(25) Morita, A.; Hynes, J. T. *Chem. Phys.* **2000**, *258*, 371.
(26) Rame, E. *J. Colloid Interface Sci.* **1997**, *185*, 245.
(27) Davies, J. T.; Rideal, E. K. *Interfacial Phenomena*, 2nd ed.; Academic Press: New York, 1963.
(28) Watry, M.; Richmond, G. L. *J. Am. Chem. Soc.* **2000**, *122*, 875.
(29) Lai, J. T.; Lau, F. W.; Robb, D.; Westh, P.; Nielsen, G.; Trandum, C.; Hvidt, A.; Koga, Y. *J. Solution Chem.* **1995**, *24*, 89.
(30) Qian, X.; Han, B.; Liu, Y.; Yan, H.; Liu, R. *J. Solution Chem.* **1995**, *24*, 1183.
(31) Dabkowski, J.; Zagorska, I.; Dabkowska, M.; Koczorowski, Z.; Trasatti, S. *J. Chem. Soc., Faraday Trans.* **1996**, *92*, 3873.
(32) Watry, M. R.; Tarbuck, T. L.; Richmond, G. L. *J. Phys. Chem. B* **2003**, *107*, 512.
(33) Goates, S. R.; Schofield, D. A.; Bain, C. D. *Langmuir* **1999**, *15*, 1400.
(34) Knock, M. M.; Bell, G. R.; Hill, E. K.; Turner, H. J.; Bain, C. D. *J. Phys. Chem. B* **2003**, *107*, 10801.
(35) Gragson, D. E.; Richmond, G. L. *J. Phys. Chem.* **1998**, *102*, 3847.
(36) Durig, J. R.; Griffin, M. G. *J. Chem. Phys.* **1977**, *67*, 2220.
(37) Allkins, J. R.; Hendra, P. J. *Spectrochim. Acta* **1966**, *22*, 2075.
(38) Ziolek, M.; Saur, O.; Lamotte, J.; Lavalley, J.-C. *J. Chem. Soc., Faraday Trans.* **1994**, *90*, 1029.
(39) Levin, I. W.; Pearce, A. R.; Spiker, R. C. J. *Spectrochim. Acta* **1975**, *31A*, 41.
(40) Klaeboe, P. *Acta Chem. Scand.* **1968**, *22*, 2817.
(41) Remizov, A. B.; Fishman, A. I.; Pominov, I. S. *Spectrochim. Acta* **1977**, *35A*, 901.
(42) Forel, M.-T.; Tranquile, M. *Spectrochim. Acta* **1970**, *26A*, 1023.
(43) Ling, Y.-C.; Vickers, T. J.; Mann, C. K. *Appl. Spectrosc.* **1985**, *39*, 463.
(44) McLachlan, R. D.; Carter, V. B. *Spectrochim. Acta* **1969**, *26A*, 1121.
(45) Mizuno, K.; Imafuji, S.; Ochi, T.; Ohta, T.; Maeda, S. *J. Phys. Chem.* **2000**, *104*, 11001.
(46) Adachi, D.; Katsumoto, Y.; Sato, H.; Ozaki, Y. *Appl. Spectrosc.* **2002**, *56*, 357.
(47) Mrazkova, E.; Hobza, P. *J. Phys. Chem. A* **2003**, *107*, 1032.
(48) Scheiner, S.; Grabowski, S. J.; Kar, T. *J. Phys. Chem. A* **2001**, *105*, 10607.
(49) Alabugin, I. V.; Manoharan, M.; Peabody, S.; Weinhold, F. *J. Am. Chem. Soc.* **2003**, *125*, 5973.
(50) Hermansson, K. *J. Phys. Chem. A* **2002**, *106*, 4695.
(51) Qian, W.; Krimm, S. *J. Phys. Chem. A* **2002**, *106*, 6628.
(52) Scheiner, S.; Kar, T. *J. Phys. Chem. A* **2002**, *106*, 1784.
(53) Li, X.; Liu, L.; Schlegel, H. B. *J. Am. Chem. Soc.* **2002**, *124*, 9639.
(54) Karpovich, D. S.; Ray, D. *J. Phys. Chem. B* **1998**, *102*, 649.
(55) Baldelli, S.; Schnitzer, C.; Shultz, M. J.; Campbell, D. J. *J. Phys. Chem. B* **1997**, *49*, 10435.
(56) Du, Q.; Superfine, R.; Freysz, E.; Shen, Y. R. *Phys. Rev. Lett.* **1993**, *70*, 2313.
(57) Scherer, J. R. The Vibrational Spectroscopy of Water. In *Advances in Infrared and Raman Spectroscopy*; Clark, R. J. H., Hester, R. E., Eds.; Heyden: Philadelphia, 1978; Vol. 5; p 149.
(58) Scherer, J. R. *J. Phys. Chem.* **1974**, *78*, 1304.
(59) Walrafen, G. E.; Hokmabadi, M. S.; Yang, W.-H. *J. Chem. Phys.* **1986**, *85*, 6964.
(60) Walrafen, G. E.; Fisher, M. R.; Hokmabadi, M. S.; Yang, W.-H. *J. Chem. Phys.* **1986**, *85*, 6970.
(61) Wei, X.; Shen, Y. R. *Phys. Rev. Lett.* **2001**, *86*, 4799.
(62) Steinbach, C.; Andersson, P.; Kazimirski, J. K.; Buck, U.; Buch, V.; Beu, T. A. *J. Phys. Chem. A* **2004**, *108*, 6165.
(63) Andersson, P.; Steinbach, C.; Buck, U. *Eur. Phys. J. D* **2003**, *24*, 53.
(64) Pribble, R. N.; Zwier, T. S. *Science* **1994**, *265*, 75.
(65) Wilson, K. R.; Cavalleri, M.; Rude, B. S.; Schaller, R. D.; Nilsson, A.; Pettersson, L. G. M.; Goldman, N.; Catalano, T.; Bozek, J. D.; Saykally, R. J. *J. Phys.: Condens. Matter* **2002**, *14*, L221.
(66) Vassilev, P.; Hartnig, C.; Koper, M. T. M.; Frechard, F.; van Santen, R. A. *J. Chem. Phys.* **2001**, *115*, 9815.

(67) Wilson, K. R.; Schaller, D. T. C.; Saykally, R. J.; Rude, B. S.; Catalano, T.; Bozek, J. D. *J. Chem. Phys.* **2002**, *117*, 7738.
(68) Dang, L. X.; Chang, T.-M. *J. Chem. Phys.* **1997**, *106*, 8149.
(69) Gragson, D. E.; Richmond, G. L. *J. Am. Chem. Soc.* **1998**, *120*, 366.
(70) Borin, I. A.; Skaf, M. S. *J. Chem. Phys.* **1999**, *110*, 6412.
(71) Soper, A. K.; Luzar, A. *J. Phys. Chem.* **1996**, *100*, 1357.
(72) Skaf, M. S. *J. Phys. Chem.* **1999**, *103*, 10719.
(73) Luzar, A.; Chandler, D. *J. Chem. Phys.* **1993**, *98*, 8160.
(74) Scatena, L. F.; Richmond, G. L. *Chem. Phys. Lett.* **2004**, *383*, 491.
(75) Scherer, J. R.; Go, M. K.; Kint, S. *J. Phys. Chem.* **1973**, *77*, 2108.